State-Dependent Solvation of Pyrene in Supercritical CO_2

Jeanette K. Rice, Emily D. Niemeyer, Richard A. Dunbar, and Frank V. Bright*

Contribution from the Department of Chemistry, Natural Science and Mathematics Complex, State University of New York at Buffalo, Buffalo, New York 14260-3000

Received January 9, 1995[⊗]

Abstract: We experimentally address the issue of solute-fluid and solute-solute interactions in dilute supercritical solutions. Using the fluorescent probe pyrene, we carry out a detailed spectroscopic study of pyrene-pyrene and pyrene-fluid interactions as a function of CO_2 density. UV-vis absorbance and steady-state fluorescence experiments confirm that the excimer-like emission seen for pyrene is not the result of soluble pyrene aggregates nor does it result from detectable, dissolved ground-state pyrene species. The extent of local density enhancement surrounding pyrene molecules is also independent (within experimental error) of pyrene concentration for the ground- and excited-state species, indicating that the pyrene molecules are solvated individually, not in pairs or higher aggregates. The magnitude of local density enhancement surrounding an excited-state pyrene molecule is, however, 1.5 times that of the ground-state pyrene species. This particular result is in excellent agreement with predictions based on the electrostatic interaction energy of ground- and excited-state pyrene with CO_2. Together these results provide strong evidence against dissolved ground-state solute-solute preassociation between pyrene molecules in CO_2 and provides the first experimental evidence on state-dependent local density enhancements in dilute supercritical fluid solutions.

Introduction

Supercritical fluids present unique features which have made them the subject of much research and led to their use in areas ranging from chromatography[1,2] and extractions[3,4] to chemical reactions.[5-11] Unfortunately, the use of supercritical fluids has actually outpaced our understanding of intermolecular solute-fluid and solute-solute interactions in dilute supercritical fluid solutions.[12-16]

Over a decade ago, Eckert and co-workers[17] measured solute partial molar volumes of naphthalene in ethylene and found that the values were extremely large and negative, indicating a "collapsing" of the fluid around the solute. This seminal work lead to the concept that as a dilute mixture approached its critical point, the *local* environment (i.e., the cybotactic region) surrounding dissolved solute molecules deviated substantially compared to the bulk properties of the fluid. This intriguing phenomenon has been termed "molecular charisma",[18] "density augmentation",[19] or "fluid clustering".[20] The reader is directed to several edited volumes and recent papers that summarize the experimental and computational work in this area.[12-16,21-29]

Kurnick et al.[30] reported that the solubility of a solute in a supercritical fluid is significantly enhanced by the presence of a second solute. That is, there can be a synergism between solutes in supercritical mixtures. The extent and magnitude of this solute-solute interaction too has been studied using spectroscopy and computational methods.[12-16,21-28] Many of the experimental reports on solute-solute clustering in supercritical fluids[31-33] used pyrene as the solute because it is a chromophore, it is fluorescent, and its photophysics have been

* Author to whom all correspondence should be addressed. (716)645-6800 ext. 2162 (office); (716) 645-6963 (FAX); CHEFVB@UBVMS.CC.BUFFALO.EDU (e-mail).

⊗ Abstract published in *Advance ACS Abstracts*, May 15, 1995.

(1) *Supercritical Fluid Chromatography*; Smith, R. M., Ed.; Royal Society of Chemistry Monograph: London, U.K., 1988.
(2) Smith, R. D.; Wright, B. W.; Yonker, C. R. *Anal. Chem.* **1988**, *60*, 1323A.
(3) McHugh, M. A.; Krukonis, V. J. *Supercritical Fluid Extraction-Principles and Practice*; Butterworths: Boston, MA, 1993.
(4) Chester, T. L.; Pinkston, J. D.; Raynie, D. E. *Anal. Chem.* **1994**, *66*, 106R.
(5) Johnston, K. P.; Haynes, C. *AIChE J.* **1987**, *33*, 2017.
(6) Kim, S.; Johnston, K. *Ind. Eng. Chem. Res.* **1987**, *26*, 1206.
(7) Randolph, T. W.; Carlier, C. *J. Phys. Chem.* **1992**, *96*, 5146.
(8) Kaupp, G. *Angew. Chem., Int. Ed. Engl.* **1994**, *33*, 1452.
(9) (a) Roberts, C. B.; Zhang, J.; Chateauneuf, J. E.; Brennecke, J. F. *J. Am. Chem. Soc.* **1993**, *115*, 9576. (b) Roberts, C. B.; Zhang, J.; Brennecke, J. F.; Chateauneuf, J. E. *J. Phys. Chem.* **1993**, *97*, 5618.
(10) DeSimone, J. M.; Maury, E. E.; Menceloglu, Y. Z.; McClain, J. B.; Romack, T. J.; Combes, J. R. *Science* **1994**, *265*, 356.
(11) Scholsky, K. M. *J. Supercrit. Fluids* **1993**, *6*, 103.
(12) Pfund, D. M.; Zemanian, T. S.; Linehan, J. C.; Fulton, J. L.; Yonker, C. R. *J. Phys. Chem.* **1994**, *98*, 11846.
(13) *Supercritical Fluid Science and Technology*; Johnston, K. P., Penninger, J. M. L., Eds. ACS Symposium Series; American Chemical Society: Washington, DC, 1989; Vol. 406.
(14) *Supercritical Fluid Technology-Reviews in Modern Theory and Applications*; Bruno, T. J., Ely, J. F., Eds.; CRC Press: Boca Raton, FL, 1991.
(15) *Supercritical Fluid Technology-Theoretical and Applied Approaches in Analytical Chemistry*; Bright, F. V., McNally, M. E. P., Eds.; ACS Symposium Series; American Chemical Society: Washington, DC, 1992; Vol. 488.
(16) *Supercritical Fluid Engineering Science-Fundamentals and Applications*; Kiran, E., Brennecke, J. F., Eds.; ACS Symposium Series; American Chemical Society: Washington, DC, 1993; Vol. 514.
(17) Eckert, C. A.; Ziger, D. H.; Johnston, K. P.; Ellison, T. K. *Fluid Phase Equilib.* **1983**, *14*, 167.
(18) Eckert, C. A.; Knutson, C. A. *Fluid Phase Equilib.* **1993**, *83*, 93.
(19) Brennecke, J. F.; Tomasko, D. L.; Peshkin, J.; Eckert, C. A. *Ind. Eng. Chem. Res.* **1990**, *29*, 1682.
(20) Kim, S.; Johnston, K. P. *AIChE J.* **1987**, *33*, 1603.
(21) Sun, Y.-P.; Fox, M. A. *J. Phys. Chem.* **1993**, *97*, 282.
(22) Fox, M. A.; Sun, Y.-P. *Pure Appl. Chem.* **1993**, *65*, 1713.
(23) Eckert, C. A.; Bergmann, D. L.; Tomasko, D. L.; Ekart, M. P. *Acc. Chem. Res.* **1993**, *26*, 621.
(24) (a) Schulte, R. D.; Kauffman, J. F. *J. Phys. Chem.* **1994**, *98*, 8793. (b) Schulte, R. D.; Kauffman, J. F. *Appl. Spectrosc.* **1995**, *49*, 31.
(25) Sun, Y.-P.; Bunker, C. E. *J. Chem. Soc., Chem. Commun.* **1994**, 5.
(26) Sun, Y.-P.; Bowen, T. L.; Bunker, C. E. *J. Phys. Chem.* **1994**, *98*, 12486.
(27) Rice, J. K.; Christopher, S. J.; Narang, U.; Peifer, W. R.; Bright, F. V. *Analyst* **1994**, *119*, 505.
(28) Munoz, F.; Chimowitz, E. H. *J. Chem. Phys.* **1993**, *99*, 5450
(29) Chialvo, A.; Cummings, P. T. *AIChE J.* **1994**, *40*, 1558.
(30) Kurnick, R. T.; Holla, S. J.; Reid, R. C. *Fluid Phase Equilib.* **1982**, *8*, 93.
(31) Brennecke, J. F.; Tomasko, D. L.; Eckert, C. A. *J. Phys. Chem.* **1990**, *94*, 7692.
(32) Zagrobelny, J.; Betts, T. A.; Bright, F. V. *J. Am. Chem. Soc.* **1992**, *114*, 5249.
(33) Zagrobelny, J.; Bright, F. V. *J. Am. Chem. Soc.* **1992**, *114*, 7821.

0002-7863/95/1517-5832$09.00/0

investigated in liquids,[34-36] at interfaces,[37,38] and in organized media.[39] In normal liquids, pyrene can form an excited-state dimer (excimer) that is generally observed when the pyrene concentration exceeds ca. 10^{-3} M.[34] In supercritical fluids, Brennecke et al.[31] first observed excimer-like emission at pyrene concentrations in the micromolar range and attributed this to an increase in pyrene−pyrene interactions (i.e., solute−solute clustering) in proximity to the fluid critical point. Zagrobelny et al.[32] confirmed this excimer-like emission in supercritical fluids at concentrations lower than those observed for liquids, thereby supporting the conclusion that some aspect of the fluid leads to an increase in excimer-like emission. However, static emission and excitation spectra[32,33,40] over a broad temperature and pressure range were consistent with a homogeneous pyrene ground state;[41] no evidence for any form of preassociated pyrene in the ground state was detectable. Time-resolved fluorescence showed[32,33,40] that the excimer-like emission was indeed due to an excited-state dimer, and this formation step was essentially diffusion controlled in supercritical fluids.[42] Thus, the excimer emission seen previously[31] in the supercritical fluids arises because pyrene molecules can simply diffuse more rapidly in the supercritical fluids. Other more recent work has shown that nearly all systems that are diffusion controlled in normal liquids also follow diffusion control in supercritical fluids.[9,43]

In this journal, Sun[44] recently reported on pyrene in supercritical CO_2 and suggested a supercritical fluid-assisted solute−solute clustering mechanism. Sun studied a single pyrene concentration (20 μM) and investigated the absorbance and fluorescence in supercritical CO_2 at $T = 45$ °C over a wide density range. Sun observed pyrene excimer-like emission at a reduced density ($\varrho_r = \varrho_{exp}/\varrho_{crit}$; ϱ_{exp} = experimental density and ϱ_{crit} = critical density) of 0.282 and concluded that two solvent environments exist about dissolved pyrene molecules and that efficient excimer formation results from the pyrene molecules which are better solvated.[44] In other words, Sun's work provided evidence suggesting that more than one pyrene molecule is included within a fluid cluster, and it is this close proximity of the two pyrene molecules which allows, in part, excimer formation at lower fluid densities. However, this result runs somewhat counter to previous results from our laboratory[32,33,40,42] and other results on diffusion control reactions.[9,43]

In this paper, we present new results on pyrene in supercritical CO_2 which show there are no ground-state solute−solute interactions for dissolved pyrene in supercritical CO_2. We also compare, for the first time, the extent of local density enhancement surrounding ground- and excited-state pyrene molecules in supercritical CO_2.

Results and Discussion

Pyrene−Pyrene Interactions. Molecules generally absorb radiation of energy that matches the energy of specific molecular transitions.[45] As a result, electronic absorbance spectra can serve to identify molecular species on the basis of the location of their absorbance bands. For example, ground-state pyrene−pyrene species, if they form, would result in detectable changes in the pyrene electronic absorbance spectrum.[41] Sun reported a new band at the red edge of the absorbance spectrum of 20 μM pyrene in CO_2 at low fluid densities and found that this new band decreased in magnitude at higher fluid densities.[44] This new band was attributed to more than one pyrene molecule being solvated within a single CO_2 cluster.[44]

Figure 1 presents new UV−vis absorbance spectra from our laboratory of 20 μM pyrene in CO_2 at reduced densities ranging from 0.240 to 1.91. As expected, the absorbance increases with increasing fluid density and levels off at the higher densities. This arises because all the available pyrene in the cell is not soluble at the lowest fluid densities. Close inspection of these results also shows there is a shift in the spectra (*vide infra*) with density, but no new red-edge band is evident. If such a band were to form,[44] its location would be close to the point denoted by the solid vertical line.

Interestingly, at a higher pyrene concentration (e.g., 75 μM), where one experimentally observes pyrene excimer emission,[31-33,40] the electronic absorbance spectra are consistent with those for 20 μM pyrene (Figure 2). In fact, no new red-edge absorption band was observed at any of the pyrene concentrations investigated in this study (10, 20, 50, 75, and 100 μM).

Origin of Red-Edge Band and Anomalous Excimer-like Emission. This red-edge absorption band was reported previously[44] and cited as evidence of pyrene−pyrene preassociation that in turn led to efficient excimer formation. However, we failed to observe this band (Figures 1 and 2), and our previous work[32,33,40] demonstrated that excimer formation in supercritical fluids was essentially diffusion controlled.[42] Thus, there must be some other explanation behind the new band observed by Sun.[44]

All our experiments are carried out using fused silica optical windows, but other window materials are certainly available and could have been used in the work previously cited. In order to determine the effect of different window materials on the absorbance spectra, sapphire windows (Insaco, Inc., Quakertown, PA) were placed into our high-pressure cell and all the aforementioned experiments repeated. All sample preparation methods were identical to those using the fused silica windows. Figure 3 presents a series of normalized pyrene absorbance spectra acquired using sapphire windows. These particular spectra were acquired in the low-density region, where pyrene−pyrene ground-state interactions are reportedly[44] most prevalent. Clearly, as was the case with the fused silica windows, no anomalous red-edge band is observed.

It is well-known that spectra arising from surface-sorbed pyrene species differ from those seen in liquids and supercritical fluids.[41,46-50] In order to determine what effect, if any, direct

(34) Birks, J. B. *Photophysics of Aromatic Molecules*; Wiley-Interscience: New York, 1970.
(35) Forster, T. H.; Kasper, K. Z. *Z. Phys. Chem.* **1954**, *1*, 275.
(36) Birks, J. B.; Dyson, D. J.; Munro, I. H. *Proc. R. Soc. A* **1963**, *275*, 575.
(37) Lochmuller, C. H.; Wenzel, T. J. *J. Phys. Chem.* **1990**, *94*, 4230.
(38) Yamanaka, T.; Takahashi, Y.; Kitamura, T.; Uchida, K. *Chem. Phys. Lett.* **1990**, *172*, 29.
(39) Yorozu, T.; Hoshino, M.; Imamura, M. *J. Phys. Chem.* **1982**, *86*, 4426.
(40) Zagrobelny, J.; Bright, F. V. *J. Am. Chem. Soc.* **1993**, *115*, 701.
(41) Winnik, F. *Chem. Rev.* **1993**, *93*, 587.
(42) Previous reports from our laboratory[33] suggested that the pyrene excimer emission may have been *slower* in certain fluids (e.g., CF_3H) than is predicted by diffusion control. More recent, unpublished time-resolved intensity decay data from our laboratory using true single-photon detection suggest that part of the earlier "deviation" from diffusion control observed by us may simply be a result of the inadequate time resolution in our earlier work that in turn lead to our not fitting to a global minimum on the χ^2 error surfaces.
(43) O'Brien, J. A.; Randolph, T. W.; Carlier, C.; Ganapathy, S. *AIChE J.* **1993**, *39*, 1061.
(44) Sun, Y.-P. *J. Am. Chem. Soc.* **1993**, *115*, 3340.
(45) Willard, H. H.; Merritt, L. L., Jr.; Dean, J. A.; Settle, F. A., Jr. *Instrumental Methods of Analysis*, 7th ed.; Wadsworth: Belmont, CA, 1988; Chapter 7.
(46) Bauer, R. K.; de Mayo, P.; Ware, W. R.; Wu, K. C. *J. Phys. Chem.* **1982**, *86*, 3781.
(47) Fujii, T.; Shimizu, E. *Chem. Phys. Lett.* **1987**, *137*, 448.
(48) Pankasem, S.; Thomas, J. K. *J. Phys. Chem.* **1991**, *95*, 7385.
(49) de Mayo, P.; Natarajan, V.; Ware, W. R. In *Organic Phototransformations in Nonhomogenous Media*; Fox, M. A., Ed.; ACS Symposium Series 278; American Chemical Society, Washington, DC, 1985; Chapter 1.

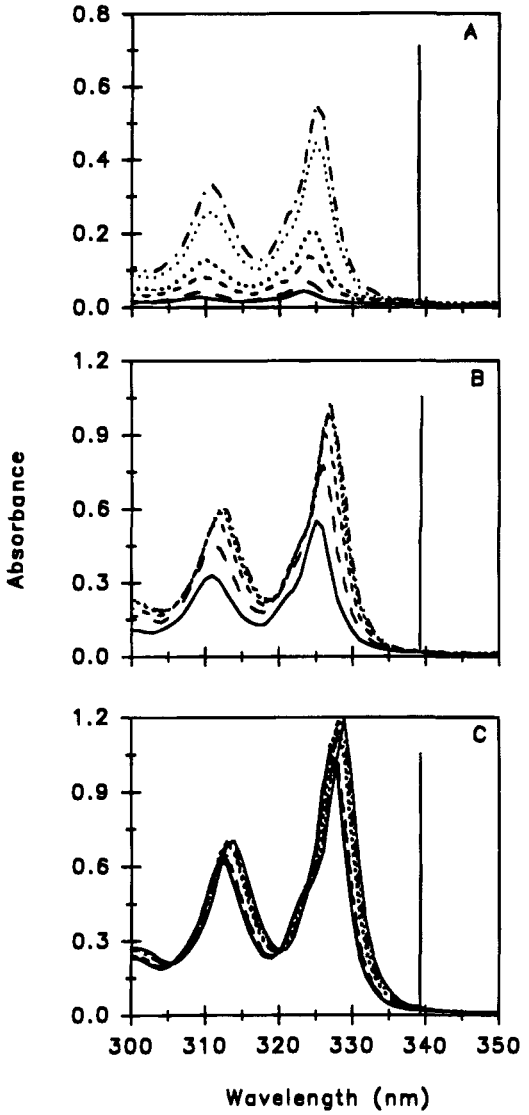

Figure 1. UV−vis absorbance spectra of 20 μM pyrene in CO_2 at 45.0 °C. (A) $\varrho_r = 0.239-0.515$; (B) $\varrho_r = 0.608-0.989$; (C) $\varrho_r = 1.08-1.91$. The vertical solid line denotes the wavelength where preassociated pyrene aggregates absorb.

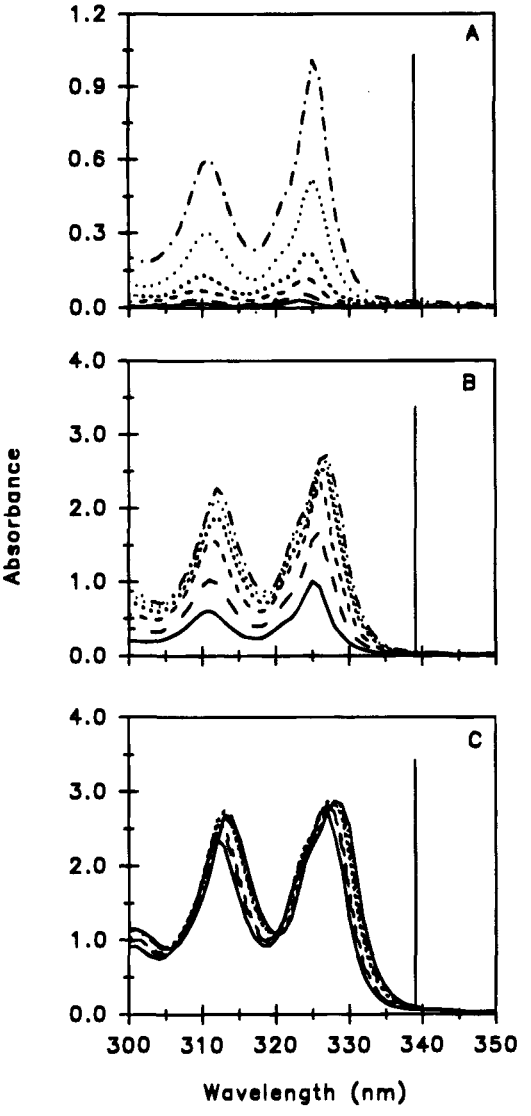

Figure 2. UV−vis absorbance spectra of 75 μM pyrene in CO_2 at 45 °C: (A) $\varrho_r = 0.239-0.515$; (B) $\varrho_r = 0.608-0.989$; (C) $\varrho_r = 1.08-1.91$. The vertical solid line denotes the wavelength where preassociated pyrene aggregates absorb.

contact of pyrene with our optical windows has on the absorbance spectra, the following experiment was performed. One of the sapphire windows was removed from the high-pressure cell, and 15 μL of 20 μM pyrene (in hexane) solution was pipetted directly onto *one* face of the sapphire window. The hexane was allowed to evaporate slowly, the window was resealed into the high-pressure cell, with the pyrene-coated surface facing *into* the cell, and the optical axis of the UV-vis spectrophotometer passed through this window. The absorbance spectra were then acquired as a function of fluid density (Figure 4). At the lowest fluid density ($\varrho_r = 0.240$) there is indeed a new band at the red edge of the spectrum. Further, as fluid density is increased, the band gradually decreases until it is no longer detectable above $\varrho_r = 0.383$. This result is consistent with the red-edge band arising from pyrene species that are physisorbed to the surface of the sapphire window. As the CO_2 density is increased, the surface-sorbed pyrene is dissolved away from the interface by the CO_2. Parallel experiments with fused silica windows (not shown) did not exhibit such a red-edge band even when dilute pyrene solutions were contacted directly with the window surface.

(50) Zilberstein, J.; Bromberg, A.; Berkovic, G. *J. Photochem. Photobiol. A: Chem.* **1994**, *77*, 69.

Sun[44] also presented steady-state fluorescence spectra of 20 μM pyrene in CO_2 at $\varrho_r = 0.282$ excited at $\lambda_{ex} = 314$ and 335 nm (where the monomer and excimer are preferentially excited, respectively). An intense broad excimer-like fluorescence was characteristic at 335 nm excitation. The results from our laboratory differ significantly. Using 325 nm excitation and fused silica windows, and without placing pyrene directly onto the windows, we observed only the characteristic five-band monomeric emission and no detectable excimer-like emission (Figure 5).

Integration of the area under the emission spectra over the regions where the monomer and excimer emit provides a convenient means to compare the excimer to monomer ratio vs ϱ_r for various concentrations of pyrene (Figure 6). Little, if any, detectable excimer emission is observed at 20 μM pyrene; however, excimer is clearly evident at higher pyrene concentrations. Examination of the actual spectra for 20 μM pyrene in supercritical CO_2 at low fluid densities (Figure 7) shows they are clearly devoid of any detectable excimer-like emission ($\lambda_{max,excimer} = 460$ nm).

On the basis of our absorbance experiments (*vide supra*), we were confident that a portion of the excimer-like emission observed by others was due in part to pyrene/surface species.

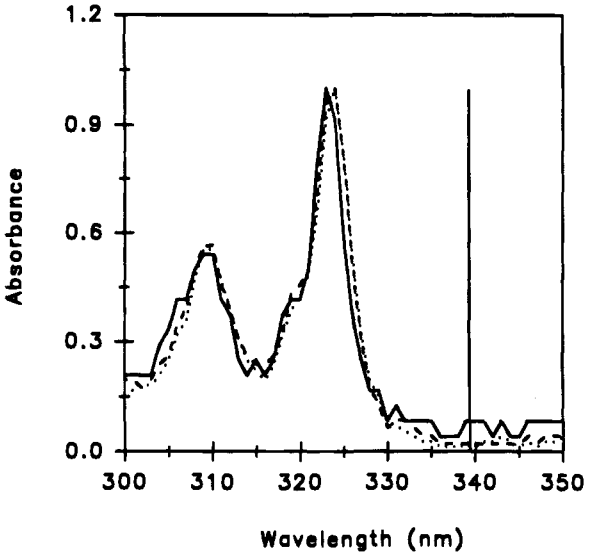

Figure 3. UV–vis absorbance spectra of 20 μm pyrene in CO_2 at 45.0 °C using sapphire windows. $\varrho_r = 0.229$ (—); 0.292 (- - -), 0.339 (-·-·-). The vertical solid line denotes the wavelength where preassociated pyrene aggregates absorb.

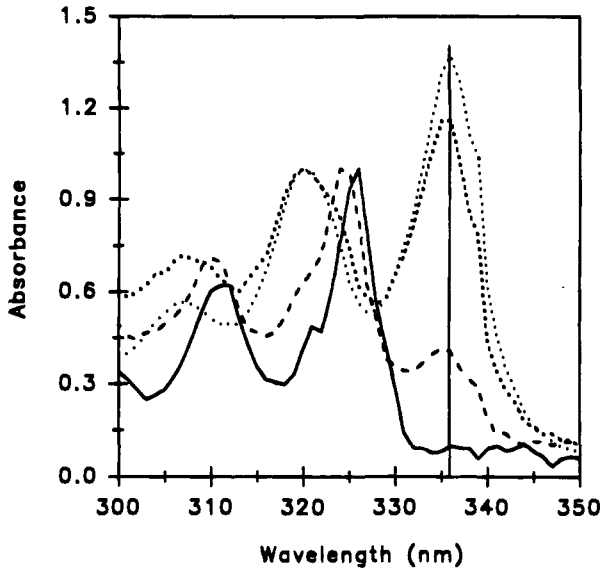

Figure 4. UV–vis absorbance spectra of pyrene physisorbed onto sapphire windows, $T = 45.0$ °C: $\varrho_r = 0.239$ (···); 0.292 (- - -); 0.339 (— — —); 0.383 (—). The vertical solid line denotes the wavelength where preassociated pyrene aggregates absorb.

However, there is also the possibility that a small fraction of the observed emission indeed arises from *solubilized* pyrene species that are preassociated and happen to form in the low-density region. Close inspection of our electronic absorbance spectra (Figure 4) and those reported by Sun[44] indicates that the pyrene "aggregates" preferentially absorb between 334 and 338 nm. Thus, there is the possibility that excitation at 325 nm simply does not excite the aggregates well.

To address this issue we used a N_2 laser ($\lambda = 337$ nm) as the excitation source. Initially we adjusted the gate width on the gated integrator to 900 ns, such that the entire fluorescence decay profile was within the gate. The monochromator (bandpass 4.0 nm) was then stepped in 1 nm increments from 350 to 600 nm. At each wavelength the gated integrator output was averaged for 50 pulses. Figure 8 presents typical normalized fluorescence spectra for 20 μM pyrene in CO_2 at the three lowest fluid densities when excited at 337 nm. Similar spectra were observed at all other fluid densities and were independent of

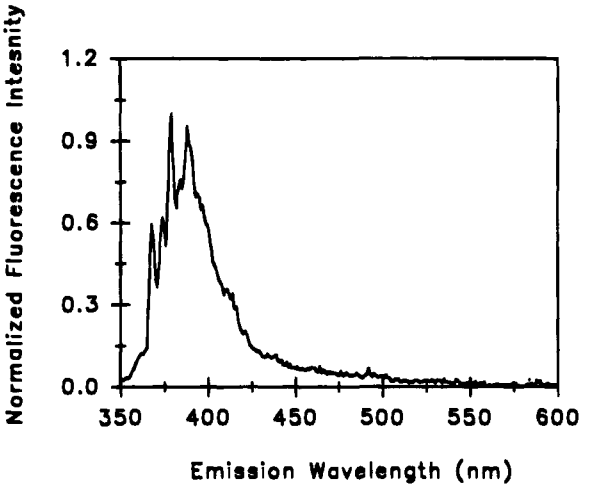

Figure 5. Normalized steady-state emission spectrum of 20 μM pyrene in CO_2. $\lambda_{ex} = 325$ nm. $\varrho_r = 0.239$. $T = 45.0$ °C.

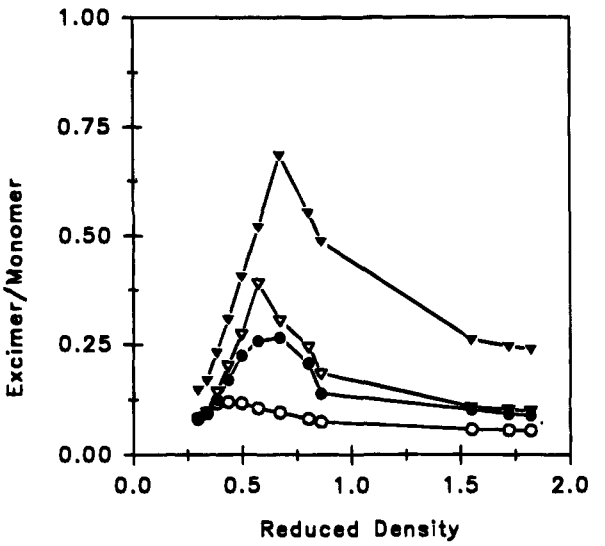

Figure 6. Recovered excimer-to-monomer ratio for 20 (○); 50 (●); 75 (▽); and 100 μM (▼) pyrene in CO_2 as a function of reduced fluid density. $\lambda_{ex} = 325$ nm. $T = 45.0$ °C.

excitation fluence. The spectral resolution is lower in Figure 8 compared to Figures 5 or 7 because of differences in emission bandpasses (4.0 vs 2.0 nm). The emission profiles may also be slightly different due to wavelength-dependent responses between individual photomultiplier tubes. However, the key features of the spectra are the clear monomer emission and the complete absence of any excimer-like emission.

If ground-state species of the form proposed by Sun[44] were present, one would expect that the emission spectra would (1) show strong excimer-like emission when excited at 337 nm and (2) differ temporally since the excited-state lifetimes of the monomer and aggregate would be different.[32,33,40,41] The previous experiment established that condition 1 is not satisfied. In order to determine whether the emission spectra were time dependent, the gated integrator width was decreased to 100 ns and its position adjusted to the peak of the intensity vs time profile (viewed on an oscilloscope) so as to monitor preferentially shorter lived species. The gate was then opened to 300 ns and delayed 400 ns, placing the gate on the region of the decay trace where longer lived species preferentially emit. Typical normalized emission spectra obtained using this time-gating scheme are presented in Figure 9. The spectral contours are essentially unchanged regardless of the region integrated,

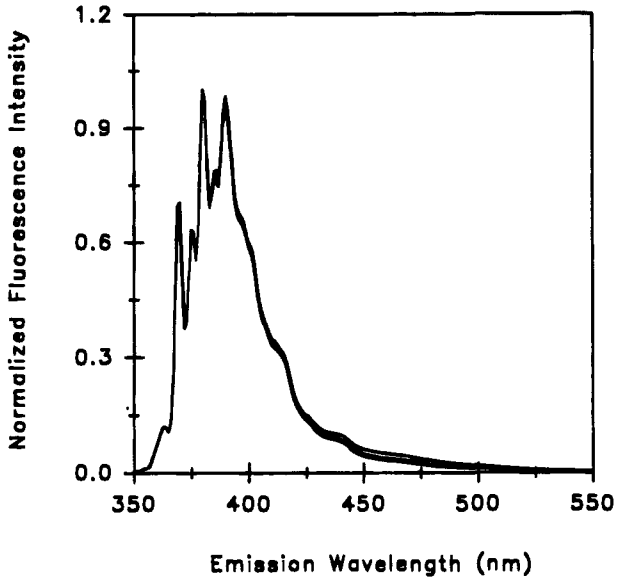

Figure 7. Normalized steady-state emission spectra of 20 μM pyrene in CO_2. $\varrho_r = 0.239$, 0.292, 0.339, and 0.383. $T = 45.0$ °C.

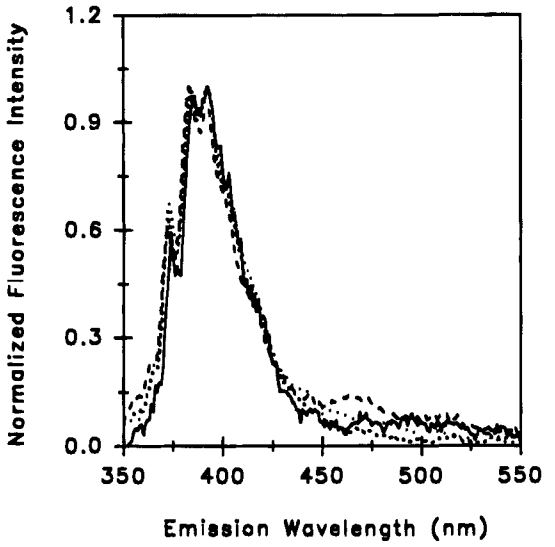

Figure 8. Normalized steady-state emission spectra acquired using the time-resolved instrument. $\lambda_{ex} = 337$ nm, $\varrho_r = 0.239$, 0.292, and 0.339. $T = 45.0$ °C.

and no excimer emission is observed. Together with the steady-state absorbance and fluorescence results (*vide supra*) we conclude there are no detectable, dissolved ground-state pyrene–pyrene species in supercritical CO_2 at these pyrene concentrations.

Local Environment Surrounding Pyrene in Supercritical CO_2. A substantial amount of literature exists on local density augmentation in supercritical fluids.[6–8,12–16,18–29] Further, there are methods available to determine the degree of density enhancement from excited-[19,51] and ground-state[20,52,53] spectra. However, in spite of these facts, there is no information on how the extent of density augmentation is affected by ground- and excited-state forms *of the same species*. In the remainder of this paper we report new results on the local environment surrounding ground- and excited-state pyrene in supercritical CO_2.

(51) Sun, Y.-P.; Bunker, C. E.; Hamilton, N. B. *Chem. Phys. Lett.* **1993**, *210*, 111.
(52) Morita, A.; Kajimoto, O. *J. Phys. Chem.* **1990**, *94*, 6420.
(53) Geldorf, P. A.; Rettschnick, R. P. H.; Hoytnick, G. J. *Chem. Phys. Lett.* **1969**, *4*, 159.

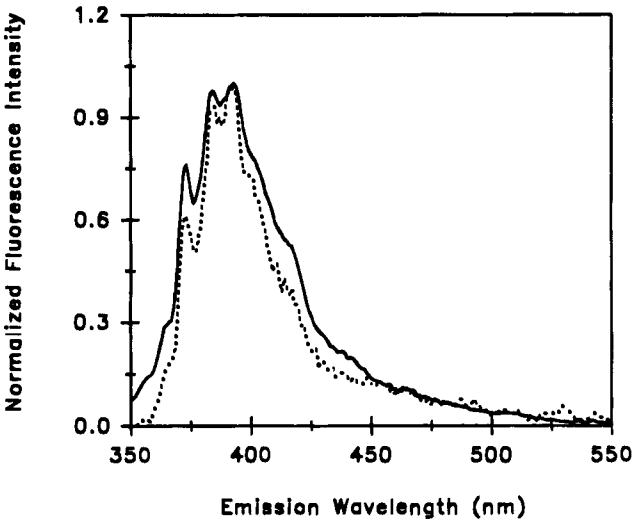

Figure 9. Normalized steady-state emission spectra of 20 μM pyrene in CO_2 acquired at short (—) and long (- - -) times following optical excitation. $\lambda_{ex} = 337$ nm. $\varrho_r = 0.339$. $T = 45.0$ °C.

Ground-State Local Density Enhancement. There are two primary types of intermolecular interactions that result in spectral changes on going from the vapor phase to solution.[34] They are *universal* interactions, which result from the solvent behaving as a dielectric medium (dependent on the dielectric constant and refractive index), and *specific* interactions, which involve the formation of hydrogen bonds, exciplexes, or other solute–solvent interactions. For the case of pyrene in CO_2, the latter is not applicable.

Universal interactions can be expressed most simply in terms of the Onsager reaction field theory (ORFT).[34] Briefly, a solute with a dipole moment, μ, contained in a spherical cavity of radius a, and dissolved in a solvent with a static dielectric constant polarizes the solvent and produces a reaction field. This reaction field lowers the ground-state energy of the solvated solute relative to the gas phase value. This shift between vapor and solution phase can be represented as[53]

$$\Delta\nu = \frac{\mu_g^2 - \mu_e^2}{a^3}\frac{n^2-1}{2n^2+1} + \frac{2\mu_e(\mu_g - \mu_e)}{a^3}\left(\frac{\epsilon-1}{\epsilon-2} - \frac{n^2-1}{n^2+2}\right) \quad (1)$$

where μ_g and μ_e are the dipole moments of the ground and excited states, respectively. ϵ and n are the bulk dielectric constant and refractive index, respectively, of the solvent.

From eq 1, for pyrene dissolved in CO_2, the frequency shift between the gas and fluid phase should be linear with the solvent polarizability term $(n^2 - 1)/(n^2 + 2)$.[21,53]

Figure 10 presents the observed bathochromic shift of pyrene in CO_2 (relative to the gas phase) as a function of solvent polarizability. The solid line represents the predicted behavior based on ORFT and was calculated using gas phase pyrene data[51] and our own experimentally determined liquid phase values. The deviation from the predicted values in the low-density region demonstrates that the local environment surrounding the ground-state pyrene molecules is different from that predicted based on bulk properties and ORFT. Specifically, in the near-critical region the local fluid environment surrounding the pyrene solute *exceeds* the expected value based on the bulk CO_2 properties. Notice also that pyrene concentration does *not* apparently affect the extent of change in the local environment surrounding the pyrene molecules.

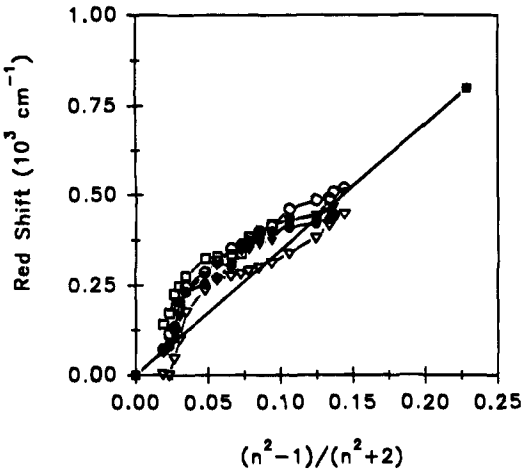

Figure 10. Effects of fluid density and pyrene analytical concentration (10, ○; 20, ●; 50, ▽; 75, ▼; and 100 μM, □) on the electronic absorbance spectra. Red shift calculated relative to the gas phase value (31 000 cm^{-1}).[54] Solid line represents predicted values based on gas phase, our experimental liquid data, and ORFT (eq 1). $T = 45.0$ °C.

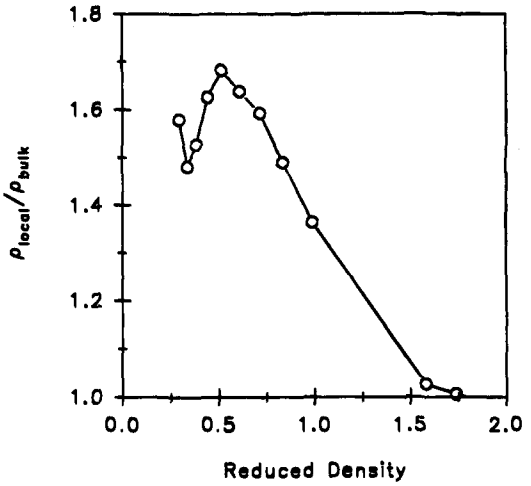

Figure 11. Recovered ground-state density enhancement ($\varrho_{local}/\varrho_{bulk}$) vs reduced fluid density for pyrene in CO_2. $T = 45.0$ °C. Data points represent the average of all pyrene concentrations.

The magnitude of the observed deviation from the bulk properties was analyzed in terms of a local CO_2 density as follows. First, computer software developed in-house and based on an extended Lorentz–Lorenz formulation[51] provides a relationship between the polarizability term $(n^2 - 1)/(n^2 + 2)$ and CO_2 density (ϱ):

$$\left(\frac{1}{\varrho}\right)\left(\frac{n^2-1}{n^2+2}\right) = 6.6 + 1.25\varrho - 264\varrho^2 \qquad (2)$$

Second, eqs 1 and 2 are used to predict the spectral shift at any *bulk* CO_2 density (ϱ_{bulk}). Finally, the actual experimental spectral shift (Figure 10) is used in concert with eq 1 to compute a *local* polarizability term that is in turn used with eq 2 to compute a *local* density (ϱ_{local}). In this manner, we are able to generate $\varrho_{local}/\varrho_{bulk}$ as a function of ϱ_r (Figure 11). The local density augmentation is a maximum at a reduced density of 0.5–0.6; the extent of density enhancement is up to 170% and decreases to unity in the high-density region. The amount of density enhancement is also apparently *not* dependent on pyrene concentration, indicating that pyrene molecules are solvated individually in CO_2.

Excited-State Local Density Enhancement. There are many techniques that can be used to determine the extent of excited-state local density enhancement.[13–16,19,51] Most applicable to our work is the "Py" scale of solvent polarity.[51,54] The monomeric emission of pyrene shows vibrational fine structure, specifically, five vibronic bands in the wavelength region between 370 and 420 nm, commonly labeled I_1, I_2, ... I_5. The pyrene I_1 transition is sensitive to the physicochemical properties of the surrounding environment (that is the intensity increases with increasing solvent polarity).[55] The intensity of the third vibronic band (I_3) is solvent independent. As a result, the ratio I_1/I_3 ("Py") serves as an indicator of local environment surrounding an excited-state pyrene molecule.[54]

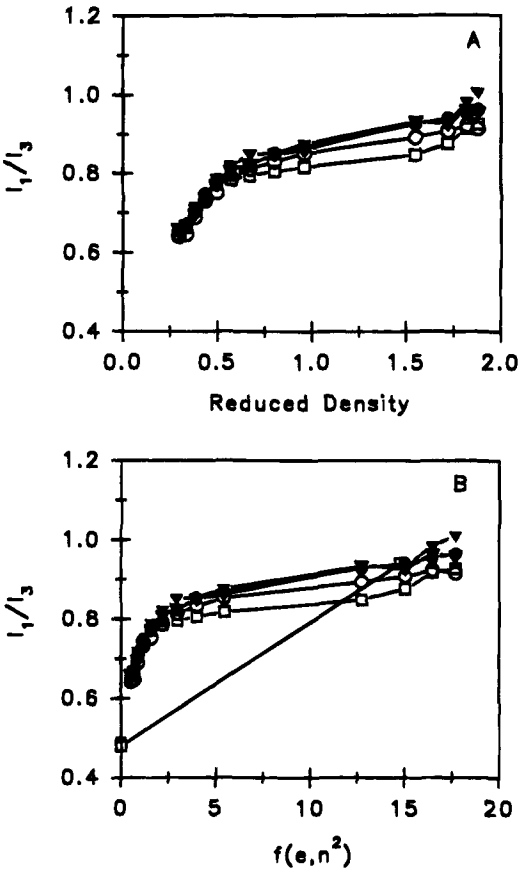

Figure 12. Effects of fluid density and pyrene analytical concentration (1, ●; 20, ▽; 50, ▼; 75, □; and 100 μM, ■) on the pyrene emission. (A) I_1/I_3 vs reduced fluid density; (B) I_1/I_3 vs solvent polarizability function. Straight line in B represents theoretical relationship dervied from gas phase and high-density liquid-like data.

From steady-state emission spectra, we were able to compare Py vs ϱ_r for various concentrations of pyrene in supercritical CO_2 (Figure 12, panel A). Consistent with previously reported results,[51] we observe an increase in Py at $\varrho_r \leq 0.50$, followed by a more gradual rise above $\varrho_r = 0.5$–0.7.

Dong and Winnik[54] established a linear correlation between the Py scale and the Kamlet, Abboud, and Taft π^* scale[55] that is based on the solvatochromic behavior of several chromophores. When solvents are broken down into classes (e.g., aprotic aliphatic, protic aliphatic, aprotic aromatic), the relationship between Py and π^* can be expressed as[51,55]

$$\text{Py} = a + b\pi^* \qquad (3)$$

where a and b are constants that depend on the solvent class. Further, π^* is linear with a function of the solvent's dielectric

(54) Dong, D. C.; Winnik, M. A. *Can. J. Chem.* **1984**, *62*, 2560.
(55) Kamlet, M. J.; Abboud, J. L.; Taft, R. W. *J. Am. Chem. Soc.* **1977**, *99*, 6027.

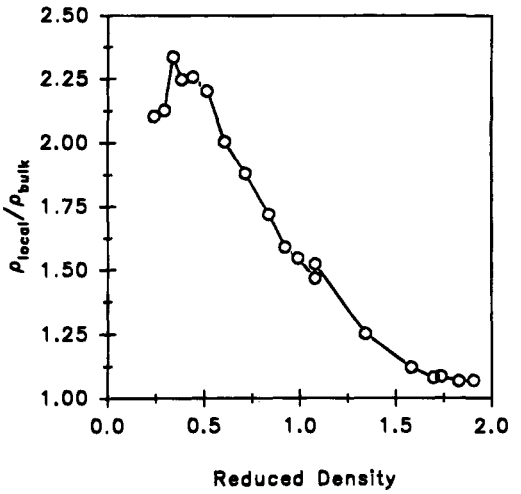

Figure 13. Excited-state density enhancement ($\varrho_{local}/\varrho_{bulk}$) vs reduced fluid density for pyrene in CO_2. $T = 45.0$ °C. Data points represent the average of all pyrene concentrations.

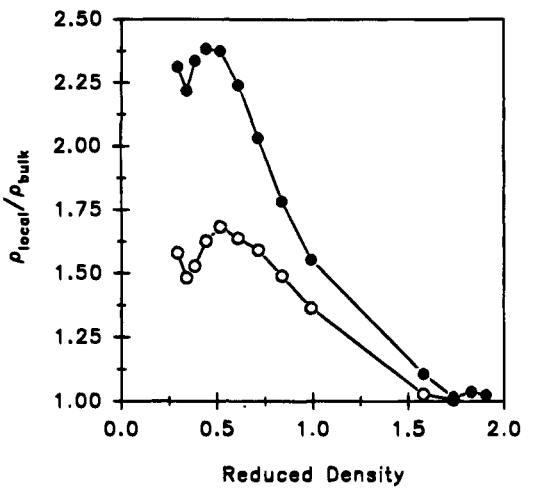

Figure 14. Comparison of ground-state (○) and excited-state (●) density enhancement for pyrene in CO_2. $T = 45.0$ °C. Data points represent the average of all pyrene concentrations.

constant and refractive index:[51,55]

$$\pi^* = c + d[f(\epsilon,n^2)] \quad (4)$$

where c and d are constants and

$$f(\epsilon,n^2) = [(\epsilon - 1)/(2\epsilon + 1)][(n^2 - 1)/(2n^2 - 1)] \quad (5)$$

On the basis on of eqs 3–5, Sun[51] suggested that the relationship between Py and $f(\epsilon,n^2)$ should also be linear in CO_2 in the absence of local density effects:

$$\text{Py} = A + B[f(\epsilon,n^2)] \quad (6)$$

In this expression A is the gas phase I_1/I_3 for pyrene (0.48) and the slope, B, is estimated from A and the Py values where local density effects are minimal (i.e., in the high-density, liquid-like region).[51]

Figure 12 (panel B) presents the pyrene I_1/I_3 vs $f(\epsilon,n^2)$, and there is clearly substantial deviation from the predicted linear behavior indicative of local changes in the environment surrounding the excited-state pyrene molecule. Several aspects of these results merit special mention. First, the deviation from the bulk is greatest in the low-density region. Second, as was observed for clustering about ground-state pyrene, the *degree* of deviation from the bulk CO_2 properties is virtually the same regardless of pyrene concentration. Using a scheme similar to that described to estimate ϱ_{local} in the ground state, we calculate $\varrho_{local}/\varrho_{bulk}$ surrounding an excited-state pyrene molecule (Figure 13). These results show that the greatest extent of density augmentation is nearly 230% at a reduced density of 0.5.

From the theoretical modeling of Chialvo and Cummings[29] for pyrene in CO_2, a plot of $\varrho_{local}/\varrho_{bulk}$ vs ϱ_r should have a maximum near $\varrho_r = 0.5$ and should decrease with increasing fluid density. Our results (Figure 14) show that the maximum deviation from the bulk properties (e.g., density) occurs between reduced densities of 0.5–0.6 in the ground and excited states. Above $\varrho_r = 0.5$–0.6 the degree of density enhancement decreases to unity, indicating that, in the high-density (liquid-like) region, local and bulk properties surrounding pyrene cease to differ.

Comparison of Density Enhancement Surrounding Ground- and Excited-State Pyrene. Recent work by Chen and McGuffin[56] provides the necessary information to make a prediction of the degree of density enhancement surrounding ground- and excited-state pyrene in supercritical CO_2. Briefly, Chen and McGuffin investigated Py in liquid and supercritical CO_2 and used semiempirical molecular orbital and molecular mechanics methods to estimate the difference in the electrostatic energy between CO_2 and pyrene in the ground and first two excited states. The pyrene ground state is totally symmetric, having ^1A_g symmetry, and the first two excited states, $^1B_{2u}$ and $^1B_{1u}$, lie very close together in energy and are closely coupled. Further, the electrostatic energies of interaction for pyrene with CO_2 in the ground and first excited state are 0.33 and 0.53 kcal/mol, respectively. The relative stability of pyrene with CO_2 is mainly controlled by dispersion forces; however, a strong electrostatic interaction exists between pyrene and CO_2.

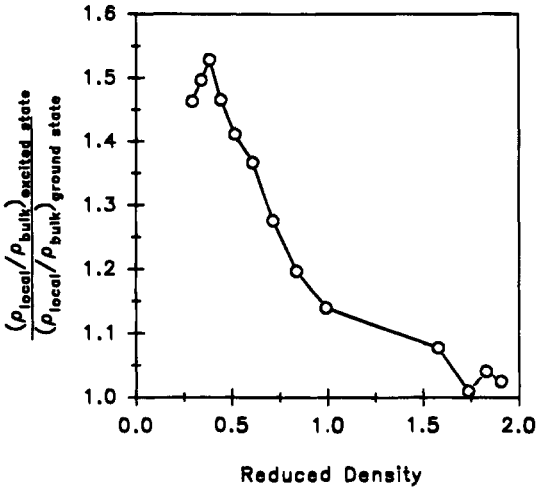

Figure 15. Ratio of excited- to ground-state density enhancement for pyrene in CO_2. $T = 45.0$ °C.

From the Chen and McGuffin work,[56] one would expect our experimental data to reveal a greater degree of local density enhancement surrounding excited-state pyrene in CO_2. Figure 14 shows that this is indeed the case. The extent of differential enhancement between the excited- and ground-state pyrene molecules is shown in Figure 15 as a plot of the ratio of enhancement factors for the excited- and ground-state pyrene vs ϱ_r. One can see clearly that the ratio is maximum near $\varrho_r = 0.5$, but approaches unity at higher densities. One should also note that the maximum in this ratio is 1.5 + 0.1, which is close to the ratio of the electrostatic energies of interaction (1.6).[56] The observed difference in the magnitude of the density enhancement between these two states can thus be accounted

(56) Chen, S.-H.; McGuffin, V. L. *Appl. Spectrosc.* **1994**, *48*, 596.

for on the basis of the electrostatic energies arising between supercritical CO_2 and ground- and excited-state pyrene molecules.

Conclusions

On the basis of the experimental results presented, we conclude there is no detectable ground-state pyrene−pyrene intermolecular interactions for dissolved pyrene molecules at low fluid densities in supercritical CO_2. This result is consistent with previous work from our group[32,33,40,42] demonstrating that pyrene excimer formation in supercritical fluids is diffusion controlled. At higher pyrene concentrations (e.g., 75 μM), where pyrene excimer is indeed observed, the excimer is only formed dynamically and there is no evidence for ground-state pyrene−pyrene pairs or higher aggregates forming in CO_2. We were able to reproduce results suggesting ground-state pyrene−pyrene interactions[44] only when pyrene was deposited directly onto the surface of a sapphire optical window. This suggests that pyrene may have been sorbed to the window surfaces in earlier experiments. It also points out the potential of using spectroscopic methods as a potentially simple and elegant means to follow dissolution of surface-adsorbed species into supercritical fluids. The magnitude of the local density enhancement is determined for the first time for ground- *and* excited-state forms of the same solute. In general, $\varrho_{local}/\varrho_{bulk}$ vs ϱ_r profiles are consistent with previous work by Knutson et al.,[57] as well as that of Randolph and co-workers.[43] The extent of augmentation about pyrene differs in the ground- and excited-state; however, within each state pyrene concentration has no detectable effect on the recovered local enhancement factors, indicating that pyrene molecules are solubilized individually. Finally, the local density enhancement in the excited state is 1.5 times greater than that in the ground state, due to increased electrostatic interaction between excited-state pyrene and CO_2. This result is in excellent agreement with reported differences in the calculated interaction energies of ground- and excited-state pyrene with CO_2.

Acknowledgment. Financial support for this research was provided by the Division of Chemical Sciences, Office of Basic Energy Sciences, Office of Energy Research, United States Department of Energy (DE-FG02-ER14143-A002).

Supplementary Material Available: Experimental details and references to pertinent literature on the instrumentation used in this work (2 pages). This material is contained in many libraries on microfiche, immediately follows this article in the microfilm version of the journal, can be ordered from ACS, and can be downloaded from the Internet; see any current masthead page for ordering information and Internet access instructions.

JA950075G

(57) Knutson, B. L.; Tomasko, D. L.; Eckert, C. A.; Debenedetti, P. G.; Chialvo, A. A. In *Supercritical Fluid Technology: Theoretical and Applied Approaches in Analytical Chemistry*; Bright, F. V., McNally, M. E. P., Eds.; ACS Symposium Series 488; American Chemical Society: Washington, DC, 1992; Chapter 5.